Received 4 August 2019; accepted 12 August 2019. Date of publication 15 August 2019; date of current version 30 August 2019.
The review of this article was arranged by Editor C. C. McAndrew.

Digital Object Identifier 10.1109/JEDS.2019.2935323

A Method for Obtaining the Real Off-State Breakdown Voltage of AlGaN/GaN MIS-HEMTs in On-Wafer Tests by Optimizing Protective Layer

SHENG GAO [1], QUANBIN ZHOU [1], XIANHUI LI [2], ZIJING XIE [2], AND HONG WANG [1,3]

1 Engineering Research Center for Optoelectronics of Guangdong Province, School of Electronics and Information Engineering, South China University of Technology, Guangzhou 510640, China
2 Engineering Research Center for Optoelectronics of Guangdong Province, School of Physics and Optoelectronics, South China University of Technology, Guangzhou 510640, China
3 Zhongshan Institute of Modern Industrial Technology, South China University of Technology, Zhongshan 528437, China

CORRESPONDING AUTHOR: H. WANG (e-mail: phhwang@scut.edu.cn)

This work was supported in part by the Science and Technologies Major Projects of Guangdong Province under Grant 2017B010112003, in part by the Applied Technologies Research and Development Projects of Guangdong Province under Grant 2015B010127013 and Grant 2016B010123004, in part by the Science and Technologies Plan Projects of Guangzhou City under Grant 201604046021 and Grant 201905010001, and in part by the Science and Technology Development Special Fund Projects of Zhongshan City under Grant 2017F2FC0002, Grant 2017A1009, and Grant 2019AG014.

ABSTRACT We demonstrate a method for testing the real off-state breakdown voltage (V_{BD}) of AlGaN/GaN metal–insulator-semiconductor high electron mobility transistor (MIS-HEMTs) in on-wafer tests. The method prevents the arcing over air at high voltage by depositing the protective layer between the pad electrodes of source and drain. The influence of materials and thickness of the protective layer on the high voltage tests of MIS-HEMTs were investigated. We found that it is helpful to obtain the real V_{BD} of the devices by increasing the thickness of the protective layer and selecting a material with a higher critical breakdown field strength. The real V_{BD} of the device with a gate-to-drain spacing of 25 μm is 1164 V when 1.5 μm SiO_2 is deposited as the protective layer, which is 141% higher than that of the value tested in air.

INDEX TERMS MIS-HEMTs, on-wafer tests, protective layer, off-state breakdown voltage, critical breakdown field strength.

I. INTRODUCTION

ALGAN/GAN high electron mobility transistors (HEMTs) on silicon (Si) substrates are expected to be using in high-temperature, high-voltage and high-power applications due to the excellent material properties, such as high electron mobility, low on-resistance, and high breakdown voltage [1]–[6]. It is vital to prepare high breakdown voltage HEMTs especially in some high-powered applications, such as radar, aerospace, and rail transportation. However, due to the early arc breakdown between the electrodes, conventional test methods sometimes fail to obtain the real off-state breakdown voltage (V_{BD}) of the devices in an air atmosphere during on-wafer tests. It is found that both the electrode spacing and the material (or gas atmosphere) between the electrodes will affect the tested V_{BD} [7]–[10]. Slade and Taylor studied the effect of electrode spacing on electrical breakdown in air atmosphere. They found that when the electrode spacing exceeds 6 μm, the breakdown voltages followed Paschen's curve for the Townsend electron avalanche process in air [11]. As for different dielectric materials, McPherson *et al.* reported that the critical breakdown field strength decreases as the dielectric constant of the material increases. According to their studies, among the four materials of SiO_2, HfSiON, Ta_2O_5, and PZT (piezoelectric ceramic transducer) between the electrodes, SiO_2 has the lowest dielectric constant but the highest breakdown voltage [12]. For different gas atmosphere between the electrodes, Husain and Nema measured the breakdown voltage under the same pressure and electrode gap in air, N_2 and SF_6. They obtained the maximum breakdown voltage in SF_6 gas atmosphere, which is compatible with the calculated Paschen's curve [13]. Some researchers also carried out the breakdown measurements of AlGaN/GaN HEMTs with the samples immersed in an inert liquid (Fluorinert) [14], [15]. Besides,

This work is licensed under a Creative Commons Attribution 4.0 License. For more information, see http://creativecommons.org/licenses/by/4.0/

the breakdown characteristics of the devices tested in compressed gases [16]–[18] or in the mixed gas [19], [20] have also been reported. But these methods increase complexity to the operation for on-wafer tests in probe station.

In this work, we investigate the electrical breakdown properties of AlGaN/GaN MIS-HEMTs with different materials of protective layer between the electrodes in order to quickly evaluate the real V_{BD} of devices during on-wafer tests. The materials include SiO_2 and SiNx, which are commonly used in industrialization and easy to obtain in the laboratory. Materials with different critical breakdown field strength and thickness were deposited as protective layer by plasma enhanced chemical vapor deposition (PECVD). As a result, the devices with suitable protective layer show great convenience in evaluating the real V_{BD} during on-wafer tests in probe station. Besides, the devices with different materials of protective layer between the electrodes do not show deterioration during testing even at 150 °C. Meanwhile, the test results for the devices with suitable protective layer between the electrodes are comparable to those tested in inert liquid (Fluorine FC-40). The MIS-HEMTs with an optimized SiO_2 as protective layer reached a real V_{BD} of 1164 V in on-wafer tests, which is 141% higher than that of the value tested in air.

II. MATERIAL AND METHODS

The AlGaN/GaN epilayer used in this work was grown by metal–organic chemical vapor deposition (MOCVD). The epitaxial structure consists of a 3.5 μm carbon-doped GaN bu?er layer, a 300 nm GaN channel, a 1 nm AlN interlayer, a 19 nm un-doped $Al_{0.23}Ga_{0.77}N$ barrier layer and a 3 nm un-doped GaN cap layer. The electron sheet density and electron mobility are 1×10^{13} cm^{-2} and 1800 cm^2/Vs, respectively by Hall measurement.

The schematic cross-sectional view of the as-fabricated GaN-on-Si MIS-HEMTs is shown in Fig. 1. The fabrication process of devices started with mesa isolation by dry etching in inductive coupled plasma (ICP) equipment. Then the ohmic metal Ti/Al/Ni/Au (20 nm/100 nm/10 nm/100 nm) was deposited by electron beam (EB) deposition and annealed at 830 °C for 1 min in N_2 ambience by rapid thermal processing (RTP). Subsequently, a 200 nm SiO_2 was deposited as passivation layer in a PECVD system. A SiNx with a thickness of 20 nm was deposited as gate dielectric layer. The gate metal was formed by depositing Ni/TiW (50 nm/250 nm) in magnetron sputtering and followed a lift-off process. After that, another 1.5 μm SiO_2 (the isolation layer) was deposited to isolate the ohmic metal and pad metal. The contact window was opened by ICP and then the thick pad electrode was formed by depositing Ti/Al/Ti/Au (150 nm/600 nm/150 nm/250 nm). Next, the protective layer was deposited by PECVD in order to obtain the real V_{BD}. Finally, the thick pad electrode contact window was opened by ICP etching, and the size of the lithography opening pattern is smaller than the pad metal.

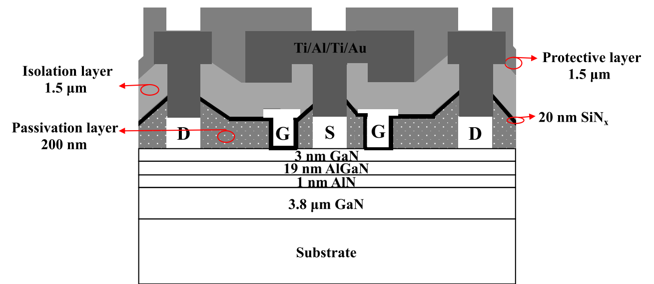

FIGURE 1. Schematic cross-section of AlGaN/GaN MIS-HEMTs.

TABLE 1. The materials and thickness of the protective layer deposited by PECVD.

Samples	A	B	C	D	E	F	G
Protective layer	Air	SiO_2	SiO_2	SiO_2	SiO_2	SiN_x	SiO_2
Thickness(μm)	0	0.2	1	1.5	3	1.5	3
Dielectric constant	1	3.9	3.9	3.9	3.9	6.8	5.4
Critical breakdown field strength* (MV/cm)	0.03	10	10	10	10	6.7	8.5
V_{BD}*(V)	482	629	928	1164	1127	818	984
Standard deviation*	29	45	72	83	79	92	69

Note: The critical breakdown field strength* was measured by plane-parallel capacitor and the V_{BD}* in the table refers to the average value. The last line in the table is the standard deviation* of V_{BD} for each sample. The total number of each sample is 30 and the L_{gd} of all samples in the table is 25 μm.

In this work, we set up seven kinds of samples to study the influence of materials and thickness of the protective layer on V_{BD} of MIS-HEMTs during on-wafer tests. All samples have similar structure expect for the protective layer as shown in table 1. Different materials growth is achieved by controlling the flow ratio of the gases and the pressure of the chamber with a deposition temperature at 300 °C. The space of gate-to-source (L_{gs}) of all samples is 5 μm and each sample has three gate-to-drain spacing (L_{gd}) of 15 μm, 20 μm and 25 μm. The length of source-field-plate and gate-field-plate of each sample are 12.5 μm and 1 μm. Meanwhile, the gate width and length of each sample are 400 μm and 3 μm, respectively. Direct-Current (DC) characterization and high voltage on-wafer tests is carried out in Cascade T200 probe station and Agilent B1505A semiconductor device analyzer in air.

III. RESULTS AND DISCUSSION

Fig. 2 shows the DC output characteristics and transfer characteristics of sample D. Besides, other samples have the same DC output characteristics and transfer characteristics as sample D, which is not shown here. The threshold voltage (V_{th}) of all samples is −3.5 V at the drain-source voltage (V_{DS}) of 15 V. The current density (I_{DS}) of the device is 450 mA/mm when the gate-source voltage (V_{GS}) is 5 V.

Fig. 3a plots the breakdown characteristics of different samples. The three-terminal off-state breakdown measurements were carried out in air and the gate is biased in pinch-off ($V_{GS} = -6$ V). We define V_{BD} as the voltage at which the I_{DS} changes abruptly as shown in Fig. 3a and the off-state current ($I_{dleakage}$) in this paper is defined as

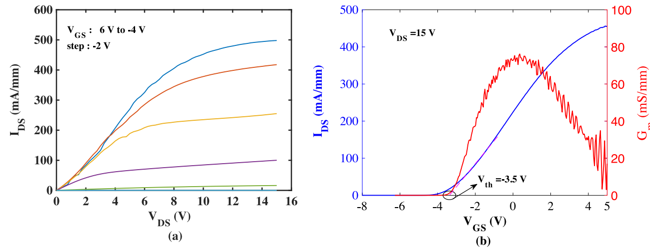

FIGURE 2. (a) DC output characteristics and (b) transfer characteristics of sample D. The L_{gd} is 25 μm.

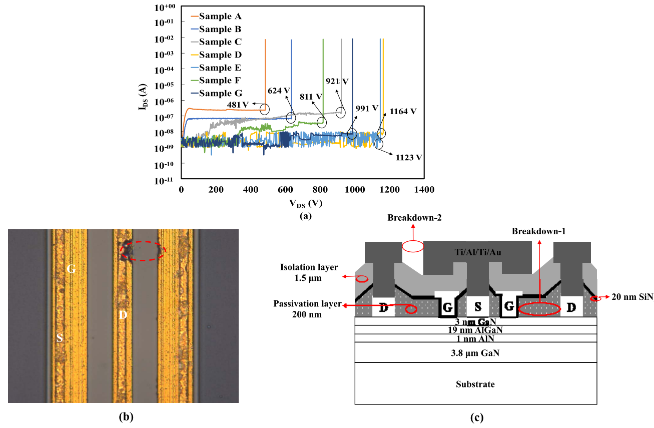

FIGURE 3. (a) Breakdown characteristics for different samples. (b) the microscope image after devices breakdown. (c) the breakdown path analysis of the devices. The L_{gd} is 25 μm.

the corresponding I_{DS} at the turning point of the breakdown curve. It is found that samples with different protective layer show significant difference in tested V_{BD} of devices. This phenomenon means that both materials and thickness of the protective layer affect the tested value of V_{BD} in MIS-HEMTs.

Fig. 3b and Fig. 3c show the microscope image after devices breakdown and the breakdown path analysis of the devices. As shown in Fig. 3b, the breakdown area in all samples occurs between the pad electrodes of source and drain but not between the gate and drain, which is different from conventional HEMTs in breakdown area [21]–[24]. From the perspective of electric field, the introduction of the field plate structure changes the electric field distribution at off-state in MIS-HEMTs and suppresses the electric field on the surface of the AlGaN barrier layer. Therefore, the breakdown area shifts from Breakdown-1 to Breakdown-2 in these samples as shown in Fig. 3c. As a result, samples with different protective layer have different tested V_{BD}. When the protective layer is not deposited, the tested V_{BD} of the device is relatively low with only 482 V.

We first compared the tested V_{BD} of samples with different thickness of the protective layer and different L_{gd}. As shown in Fig. 4a, the tested V_{BD} increase first and then saturate as the thickness of protective layer increases under the same L_{gd}. Besides, when the thickness of protective layer

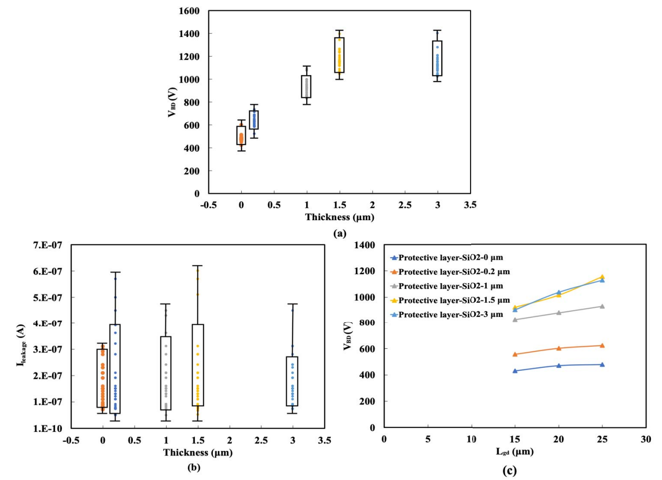

FIGURE 4. (a) The tested V_{BD} and (b) the $I_{dleakage}$ versus the thickness of the protective layer for sample A - E with L_{gd} of 25 μm. (c) the tested V_{BD} versus the L_{gd} and the thickness of the protective layer for sample A - E.

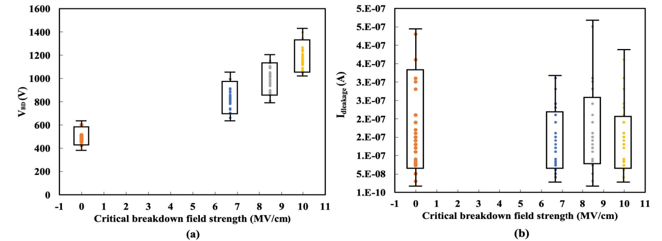

FIGURE 5. (a) The tested V_{BD} and (b) the $I_{dleakage}$ versus critical breakdown field strength of different materials for sample A, D, F, G. The L_{gd} is 25 μm.

is lower than a certain value, the tested V_{BD} nearly do not change with L_{GD}, as shown in Fig. 4c. However, the tested V_{BD} increases with the increasing of L_{GD} as the thickness exceeding 1.5 μm, which means that the protective layer plays a role in preventing the arcing over air. According to Fig. 4b, we also observed that the thickness of the protective layer has little effect on the $I_{dleakage}$ and the value of the $I_{dleakage}$ is basically kept at an order of magnitude.

In the second step, we studied the effect of materials of protective layer on the tested V_{BD}. The tested V_{BD} of sample A, sample D, sample F and sample G are shown in Fig. 5a. According to Fig. 5a, the samples with a larger critical breakdown field strength in protective layer have a higher tested V_{BD}. Moreover, the difference in materials of protective layer do not affect the $I_{dleakage}$ as shown in Fig. 5b.

To initially evaluate the impact of the protective layer used on devices reliability, we compared the breakdown characteristics of sample D at different temperatures. As show in Fig. 6a, we observed that the devices maintain good breakdown characteristics without significant deterioration even at 150 °C. These deposition processes of the protective layers are the basic processes in devices fabrication and the reliability of the devices will not be deteriorated. Besides, we

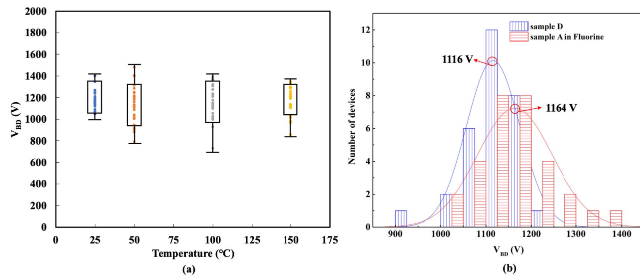

FIGURE 6. (a) The breakdown characteristics of sample D at different temperatures, (b) the tested V_{BD} of sample D with 1.5 μm protective layer and sample A in Fluorine. The L_{gd} is 25 μm.

tested sample A in inert liquid (Fluorine FC-40) solution, which is widely used in high-voltage devices testing. As shown in Fig. 6b, sample D with 1.5 μm protective layer show an average value of tested V_{BD} of 1164 V, which is comparable to that of sample A of 1116 V tested in Fluorine. In a word, samples with suitable protective layer not only show good breakdown characteristics in the comparison of samples tested in Fluorine, but also hardly have significant degradation during testing even at 150 °C.

In order to further analyze the principle of obtaining the real V_{BD} by depositing a protective layer, we propose a model to explain it. As shown in Fig. 7, the distance between the electrodes is defined as t_{act}. When a protective layer, whose thickness is smaller than that of electrodes, is deposited between the two electrodes, the t_{act} can be expressed as follow:

$$t_{act} = 2 \times t_1 + t_2 \tag{1}$$

where t_1 is the thickness of protective layer covered on the sidewall of electrodes, and t_2 is the remaining distance in air.

For the breakdown between electrodes, it is often analyzed from two aspects: the distance and the dielectric material between the electrodes. Several studies have shown that materials with smaller dielectric constant can gain higher critical breakdown field strength [7], [8], [11], [25]. For air, however, the critical breakdown field strength is more susceptible to other factors, such as air humidity and gas pressure [26]. Therefore, the tested V_{BD} of sample A obtained in air is low. Bychkov *et al.* devoted to the investigation of the critical breakdown field strength in the air, which measured about 0.03 MV/cm and even lower when considering other factors [27]. The critical breakdown field strength of SiO_2 and SiN_X is related to the process of depositing thin films [28], [29]. By adjusting the deposition process, we obtained different critical breakdown field strength, 10 MV/cm and 8.5 MV/cm of SiO_2, 6.7 MV/cm of SiNx in our laboratory.

As a result, both the distance and critical breakdown field strength of the protective layer can affect the tested V_{BD} between electrodes.

We define that the effective distance t_{eff} is the equivalent distance in air of t_{act}. The t_{act} can be converted to the t_{eff} according to the difference of the critical breakdown field strength between the protective layer and air. The specific expression of t_{eff} is as follows:

$$t'_1 \times V_{Air} = t_1 \times V_{SiO2} \tag{2}$$

$$t_{eff} = 2 \times t'_1 + t_2 \tag{3}$$

where t'_1 is the equivalent distance of t_1, V_{SiO2} and V_{Air} is the critical breakdown field strength in SiO_2 and air.

When a protective layer is deposited, the electrodes are cover by a material with high critical breakdown field strength. As the thickness of the protective layer increases, the electrodes are cover by thicker protective layer and the t_1 becomes larger. Therefore, the t_{eff} also increases. Taking sample B as an example, when the deposition thickness of SiO_2 is 0.2 μm, the t_{eff} is 152.4 μm. Then, the t_{eff} of sample B is far greater than that of sample A, which is only 19.5 μm. As a result, sample B (629 V) has a higher tested V_{BD} than sample A (482 V), which is met the classical Paschen's law. The law holds that the V_{BD} is proportional to the distance between the electrodes when the air pressure is a constant [7]–[11]. As the thickness of the protective layer increases, the t_{eff} between the electrodes becomes larger, and therefore the tested V_{BD} is improved. When the thickness of the protective layer continues to increase and exceeds the thickness of the electrodes, the space between electrodes is filled with protective layer. After that, the t_{eff} reaches the maximum value and keeps in a constant. Consequently, the tested V_{BD} reaches saturation and do not change with the increase of the thickness of the protective layer, which means that the tested V_{BD} in this case is the real V_{BD} of the devices. The results of this model are in coincident with the results in Fig. 4 (a).

On the other hand, different materials with the same thickness have different t_{eff} because of the difference in critical breakdown field strength. The t_{eff} increases with the critical breakdown field strength increasing, leading to increases of the tested V_{BD}, as the results shown in Fig. 5 (a).

IV. CONCLUSION

In this work, we prevent the arcing over air at high voltage on-wafer tests and obtained a real V_{BD} of 1164 V in AlGaN/GaN MIS-HEMTs by depositing a 1.5 μm SiO_2 on the pad electrodes of source and drain. Both the distance between the electrodes and the critical breakdown field strength of protective layer can affect the acquisition of the real V_{BD} for devices. As the thickness of the protective layer increases, the tested V_{BD} first increases and then saturates. For different materials of protective layer, materials with larger critical breakdown field strength can achieve higher tested V_{BD}. The tested V_{BD} is related to the effective distance between the electrodes, which is consistent with the theory of Paschen's law. Meanwhile, the devices with different materials of protective layer between the electrodes did not show deterioration during testing even at 150 °C. Furthermore, the test results for the devices with different materials of

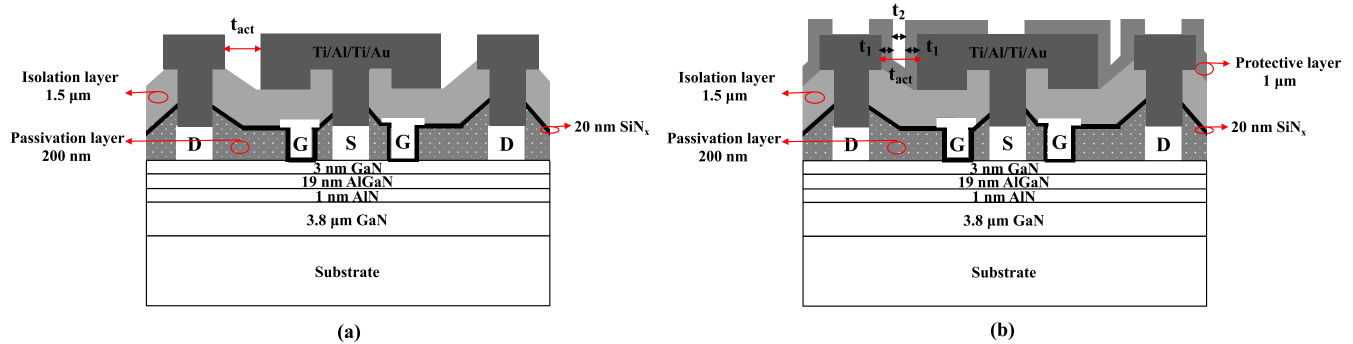

FIGURE 7. Electrodes (a) without and (b) with deposited protective layer.

protective layer between the electrodes are comparable to those tested in inert liquid (Fluorine FC-40). Our result contributes to a certain direction for obtaining the real V_{BD} of the device in high voltage on-wafer tests.

REFERENCES

[1] G. Meneghesso, M. Meneghini, and E. Zanoni, "Breakdown mechanisms in AlGaN/GaN HEMTs: An overview," *Jpn. J. Appl. Phys.*, vol. 53, no. 10, 2014, Art. no. 100211. doi: 10.7567/JJAP.53.100211.

[2] S. L. Zhao *et al.*, "Analysis of the breakdown characterization method in GaN-based HEMTs," *IEEE Trans. Power Electron.*, vol. 31, no. 2, pp. 1517–1527, Feb. 2016. doi: 10.1109/TPEL.2015.2416773.

[3] L. Zhang *et al.*, "AlGaN-channel gate injection transistor on silicon substrate with adjustable 4–7-V threshold voltage and 1.3-kV breakdown voltage," *IEEE Electron Device Lett.*, vol. 39, no. 7, pp. 1026–1029, Jul. 2018. doi: 10.1109/LED.2018.2838542.

[4] S. Cheng and P. C. Chou, "Power conditioning applications of 700V GaN-HEMTs cascode switch," in *Proc. 41st Annu. Conf. IEEE Ind. Electron. Soc. (IECON)*, Yokohama, Japan, 2015, pp. 4796–4801. doi: 10.1109/IECON.2015.7392850.

[5] X. Huang, Q. Li, Z. Liu, and F. C. Lee, "Analytical loss model of high voltage GaN HEMT in cascode configuration," *IEEE Trans. Power Electron.*, vol. 29, no. 5, pp. 2208–2219, May 2014. doi: 10.1109/Tpel.2013.2267804.

[6] X. Huang, Z. Liu, Q. Li, and F. C. Lee, "Evaluation and application of 600 v GaN HEMT in cascode structure," *IEEE Trans. Power Electron.*, vol. 29, no. 5, pp. 2453–2461, May 2014. doi: 10.1109/TPEL.2013.2276127.

[7] A. Peschot, C. Poulain, N. Bonifaci, and O. Lesaint, "Electrical breakdown voltage in micro- and submicrometer contact gaps (100nm–10μm) in air and nitrogen," in *Proc. Annu. Holm Conf. Elect. Contacts*, vol. 2015. San Diego, CA, USA, Dec. 2015, pp. 280–286. doi: 10.1109/HOLM.2015.7355110.

[8] M. Darveniza, "Electrical breakdown of air between insulated conductors," in *Proc. 6th Int. Conf. Properties Appl. Dielectric Mater.*, vol. 2. Xi'an, China, 2002, pp. 615–620. doi: 10.1109/ICPADM.2000.876090.

[9] R. S. S. Dhariwal, J.-M. Torres, and M. P. Y. Desmulliez, "Electric field breakdown at micrometre separations in air and nitrogen at atmospheric pressure," *IEE Proc. Sci. Meas. Technol.*, vol. 147, no. 5, pp. 261–265, Sep. 2000. doi: 10.1040/ip-smt:20000506.

[10] J. W. McPherson, J. Kim, A. Shanware, H. Mogul, and J. Rodriguez, "Trends in the ultimate breakdown strength of high dielectric-constant materials," *IEEE Trans. Electron Devices*, vol. 50, no. 8, pp. 1771–1778, Aug. 2003. doi: 10.1109/TED.2003.815141.

[11] P. G. Slade and E. D. Taylor, "Electrical breakdown in atmospheric air between closely spaced (0.2 µm-40 µm) electrical contacts," *IEEE Trans. Compon. Packag. Manuf. Technol.*, vol. 25, no. 3, pp. 390–396, Sep. 2002. doi: 10.1109/TCAPT.2002.804615.

[12] J. McPherson, J.-Y. Kim, A. Shanware, and H. Mogul, "Thermochemical description of dielectric breakdown in high dielectric constant materials," *Appl. Phys. Lett.*, vol. 82, no. 13, pp. 2121–2123, 2003. doi: 10.1063/1.1565180.

[13] E. Husain and R. S. Nema, "Analysis of Paschen curves for air, N2 and SF6 using the townsend breakdown equation," *IEEE Trans. Electr. Insul.*, vol. EI-17, no. 4, pp. 350–353, Aug. 1982. doi: 10.1109/TEI.1982.298506.

[14] P. Srivastava *et al.*, "Record breakdown voltage (2200 V) of GaN DHFETs on Si with 2-μm buffer thickness by local substrate removal," *IEEE Electron Device Lett.*, vol. 32, no. 1, pp. 30–32, Jan. 2011. doi: 10.1109/LED.2010.2089493.

[15] Q. Zhou *et al.*, "Schottky-contact technology in InAlN/GaN HEMTs for breakdown voltage improvement," *IEEE Trans. Electron Devices*, vol. 60, no. 3, pp. 1075–1081, Mar. 2013. doi: 10.1109/TED.2013.2241439.

[16] A. H. Cookson, "Review of high-voltage gas breakdown and insulators in compressed gas," *IEE Proc. A Phys. Sci. Meas. Instrum. Manag. Educ. Rev.*, vol. 128, no. 4, pp. 303–312, May 1981. doi: 10.1049/ip-a-1.1981.0045.

[17] A. H. Howell, "Breakdown studies in compressed gases," *Trans. Am. Inst. Elect. Eng.*, vol. 58, no. 5, pp. 193–206, May 1939. doi: 10.1109/T-AIEE.1939.5057948.

[18] A. H. Cookson, "Electrical breakdown for uniform fields in compressed gases," *Proc. Inst. Elect. Eng.*, vol. 117, no. 1, pp. 269–280, Jan. 1970. doi: 10.1049/piee.1970.0058.

[19] A. Yializis, N. H. Malik, A. H. Qureshi, and E. Kuffel, "Impulse breakdown and corona characteristics for rod-plane gaps in mixtures of SF6 and nitrogen with less than 1% of SF6 content," *IEEE Trans. Power App. Syst.*, vol. PAS-98, no. 5, pp. 1832–1840, Sep. 1979. doi: 10.1109/TPAS.1979.319501.

[20] O. Farish, S. J. Dale, and A. M. Sletten, "Impulse breakdown of positive rod-plane gaps in hydrogen and hydrogen-SF 6 mixtures," *IEEE Trans. Power App. Syst.*, vol. 95, no. 5, pp. 1639–1647, Sep. 1976. doi: 10.1109/T-PAS.1976.32263.

[21] B. Lu, E. L. Piner, and T. Palacios, "Breakdown mechanism in AlGaN/GaN HEMTs on Si substrate," in *Device Res. Conf. Dig. (DRC)*, 2010, pp. 193–194. doi: 10.1109/DRC.2010.5551907.

[22] W. Saito, T. Suwa, T. Uchihara, T. Naka, and T. Kobayashi, "Breakdown behaviour of high-voltage GaN-HEMTs," *Microelectron. Rel.*, vol. 55, nos. 9–10, pp. 1682–1686, 2015. doi: 10.1016/j.microrel.2015.06.126.

[23] C. Zhou, Q. Jiang, S. Huang, and K. J. Chen, "Vertical leakage/breakdown mechanisms in AlGaN/GaN-on-Si devices," *IEEE Electron Device Lett.*, vol. 33, no. 8, pp. 1132–1134, Aug. 2012. doi: 10.1109/Led.2012.2200874.

[24] S. Arulkumaran, S. Vicknesh, G. I. Ng, Z. H. Liu, S. L. Selvaraj, and T. Egawa, "High vertical breakdown strength in with low specific on-resistance AlGaN/AlN/GaN HEMTs on silicon," *Phys. Status Solidi Rapid Res. Lett.*, vol. 5, no. 1, pp. 37–39, 2011. doi: 10.1002/pssr.201004465.

[25] J. Chen, Y. Liu, L. Zhou, Z. Zhou, H. Mei, and T. Xie, "Electrical breakdown characteristics of air gap between conductor and tower covered by insulation sheath in 500 kV transmission line," *High Volt. Eng.*, vol. 41, no. 7, pp. 2315–2320, 2015. doi: 10.13336/j.1003-6520.hve.2015.07.027.

[26] D. Rodriguez, R. S. Gorur, and P. M. Hansen, "Effect of humidity on the breakdown characteristics of air in non-uniform fields at 30 kHz," *IEEE Trans. Dielectr. Electr. Insul.*, vol. 17, no. 1, pp. 45–52, Feb. 2010. doi: 10.1109/TDEI.2010.5412001.

[27] V. Bychkov, S. Volkov, I. Kochetov, and A. Aleksandrov, "Humid air breakdown fields in lower stratosphere," in *Proc. 50th AIAA Aerosp. Sci. Meeting Including New Horizons Forum Aerosp. Expo.*, 2014, p. 660. doi: 10.2514/6.2012-660.

[28] N. Hara, Y. Kobayashi, D. Kagaya, and N. Akao, "Formation and breakdown of surface films on magnesium and its alloys in aqueous solutions," *Corrosion Sci.*, vol. 49, no. 1, pp. 166–175, 2007. doi: 10.1016/j.corsci.2006.05.033.

[29] T. Usui, C. A. Donnelly, M. Logar, R. Sinclair, J. Schoonman, and F. B. Prinz, "Approaching the limits of dielectric breakdown for SiO2 films deposited by plasma-enhanced atomic layer deposition," *Acta Materialia*, vol. 61, no. 20, pp. 7660–7670, 2013. doi: 10.1016/j.actamat.2013.09.003.

SHENG GAO received the B.S. degree in electrical engineering and automation from Zhejiang Ocean University, Zhoushan, China, in 2016. He is currently pursuing the Ph.D. degree in miro-electronics and solid-state electronics with the South China University of Technology, Guangzhou, China.

His current research interest includes III–V nitride semiconductors and devices.

QUANBIN ZHOU received the B.S. degree in opto-electronic engineering from the Beijing Institute of Technology, Beijing, China, in 2014. He is currently pursuing the Ph.D. degree in physical electronics with the South China University of Technology, Guangzhou, China.

His current research interest includes III–V nitride semiconductors and devices.

XIANHUI LI received the B.S. degree in opto-electronic engineering from the South China University of Technology, Guangzhou, China, in 2017, where he is currently pursuing the M.S. degree in optics.

His current research interest includes III–V nitride semiconductors and devices.

ZIJING XIE received the B.S. degree in opto-electronic engineering from the South China University of Technology, Guangzhou, China, in 2018, where he is currently pursuing the M.S. degree in optics.

His current research interest includes III–V nitride semiconductors and devices.

HONG WANG received the Ph.D. degree from the South China University of Technology in 2004.

He is currently a Professor and the Doctoral Supervisor with the South China University of Technology. His research interests include micro-nano photoelectric material and device, optical communication network and devices, and GaN-based electronic materials and devices.